

QUALITY INFORMATION DOCUMENT

Black Sea Production Centre BLKSEA_ANALYSISFORECAST_BGC_007_010

Issue: 4.0

Contributors: L. Vandenbulcke, L. Macé, C. Meulders, A. Mouchet, M. Grégoire

Approval date by the CMEMS product quality coordination team:



Ref: CMEMS-BLK-QUID-007-010
Date: September 2023





Ref: Date: CMEMS-BLK-QUID-007-010

: September 2023

Issue: 4.

CHANGE RECORD

When the quality of the products changes, the QUID is updated, and a row is added to this table. The third column specifies which sections or sub-sections have been updated. The fourth column should mention the version of the product to which the change applies.

| Issue | Date | § | Description of Change | Author | Validated By |
|-------|-------------------|-----|--|--|--------------|
| 1.0 | April 2019 | All | First version for product 007_010 released at V201907 | L. Vandenbulcke, A. Capet, M. Grégoire | |
| 1.1 | May 2019 | All | Final version for qualification of 007_010 product | L. Vandenbulcke, A. Capet, M. Grégoire | E. Peneva |
| 2.0 | April 2020 | All | New version for version V202007 of the product | L. Vandenbulcke, A. Capet, M. Grégoire | E. Peneva |
| 2.1 | April 2021 | | New dataset with optical variables | L. Vandenbulcke, A. Capet, M. Grégoire | E. Peneva |
| 3.0 | August 2022 | | New version for version V202211 of the product | L. Vandenbulcke, A. Capet, L. Mace, C. Meulders, A. Mouchet, M. Grégoire | E. Peneva |
| 4.0 | September 2023 | All | New version for version V202311 | L. Vandenbulcke, L. Macé, C. Meulders, A. Mouchet, M. Grégoire | E. Peneva |





Ref:

CMEMS-BLK-QUID-007-010

Date: September 2023

Issue: 4.0

TABLE OF CONTENTS

Change Record3

Table of contents4

- I. 5
 - I.1 Products covered by this document5
- II Summary of the results6
 - II.1 Estimated Accuracy Numbers7
- III Production system description8
- III.1 Production centre details8
- III.2 Description of the production system8
- III.3 Upstream data and boundary condition of the NEMO-BAMHBI model11
- IV VAlidation framework12
- V Validation results17
 - V.1 Physical variables17
 - V.1.1 Mixed Layer Depth (MLD)17
 - V.1.2 Cold Intermediate Layer19
 - V.2 Oxygen20
 - V.3 Chlorophyll25
 - V.3.1 Satellite data25
 - V.3.2 In situ data28
 - V.4 Carbonate sub-system29
 - V.4.1 Oxygen and Nitrate29
 - V.4.2 Dissolved Inorganic Carbon30
 - V.4.3 pH and Total Alkalinity32
 - V.4.4 pC0234
 - V.5 Air-Sea CO2 Flux35
 - V.6 Optics37
 - V.6.1 Photosynthetically Active Radiation (PAR)37
 - V.6.2 Optical attenuation coefficient (Kd)39
- VI System's Noticeable events, outages or changes43
- VII Quality changes since previous version44
- VIII References44







Ref: CMEMS-BLK-QUID-007-010 Date: September 2023

Issue: 4.0

I. EXECUTIVE SUMMARY

The V202311 release of the Black Sea biogeochemical analysis-forecast uses a new version of the physical model: NEMO 4.2. that is online coupled with the Biogeochemical model for benthic and hypoxic influenced areas (BAMHBI) Compared to V2022, the vertical discretisation is changed; the 59 unevenly-spaced z-layers are coarser near the bottom, but tighter around 50-150m depth where physical and biogeochemical components present the largest gradients. The vertical and horizontal diffusion schemes are also improved, as well as the surface boundary condition. The biogeochemical model explicitly solves the chlorophyll content of each plankton functional type (PFT) and is now a state variable (as opposed to a diagnostic variable at V202211 (Geider et al, 1998). The particulate organic matter sinking velocity scheme is improved. In the data assimilation procedure of satellite chlorophyll observations, the correction is limited in depth as a function of the local mixed-layer depth.

The complete list of changes is given in section VII.

I.1 Compared to the previous version of the product (V202211), the quality of the model is improved for dissolved oxygen and for chlorophyll in the open ocean (both the surface value compared to satellites, and the vertical structure compared to BGC-ARGO). Chlorophyll on the North-Western shelf is over-estimated in summer. Nitrates are better represented in the new version. Regarding optical variables, comparison with in-situ measurements from BGC-ARGO floats reveals that normalized photosynthetically-active radiation (PAR) is slightly degraded compared to V202211, whereas the attenuation coefficient is improved. Products covered by this document

BLK_ANALYSISFORECAST_BGC_007_010 is the biogeochemical part of the Black Sea analysis-forecast system implemented by the Black Sea Marine Forecasting Centre (BLK-MFC). The online-coupled model is run with a horizontal resolution of ~2.5 km, 59 vertical levels, and generates the 6 following datasets:

- NUTR: phosphorus, nitrate
- PFTC: chlorophyll and phytoplankton biomass;
- BIOL: dissolved oxygen (O2) concentrations and net primary production;
- CARB: pH, dissolved inorganic carbon (DIC), Total Alkalinity (TA)
- CO2F: Surface partial CO₂ pressure, surface CO₂ flux
- OPT: photosynthetically active radiation (PAR) and attenuation coefficient (Kd)

The BIOL dataset also includes the bottom dissolved oxygen concentration on the North-Western Black Sea shelf, saved as a separate 2D variable.

These datasets are provided as daily, monthly and yearly means, and for some variables (I.e. CO2F) also as hourly means.

Commented [GM1]: 2.5 km?

Commented [VL2]: oui en effet





Ref: CMEMS-BLK-QUID-007-010 Date: September 2023

Issue: 4.0

II SUMMARY OF THE RESULTS

The Black Sea biogeochemical Near Real-Time product (NRT) has been validated using satellite chlorophyll time series, and *in situ* BGC-ARGO (chlorophyll, oxygen, PAR, Kd) data collected during the period 2020-2021. The other variables cannot be validated in NRT due to the absence of NRT data. They are validated in the Multi-Year product and additionally, their consistency with historical data is qualitatively checked here for inorganic nutrients, DIC, pH, pCO2, and TA.

Physics: The model version V202311 has an upgraded version of the physical forcing model (NEMO v4.2.0) compared to previous versions. The vertical resolution has been refined around the depths of the oxycline, halocline and Cold Intermediate Layer

The new model is able to simulate the mixed layer depth and cold intermediate layer (CIL) which are key physical processes governing the distribution of biogeochemical variables, water column stability and ventilation mechanisms.

Chlorophyll: Since V202007, surface chlorophyll is assimilated in the model. The product accurately represents the range of surface chlorophyll concentrations and its temporal variability. The bias is low (0.01-0.30 mg.m⁻³ depending on the region) and is very much reduced compared to the previous product version. This result is conserved in V202311, with similar EANs, e.g. bias is 0.007 to 0.88 mg.m⁻³ depending on the regions (except the region in front of the Danube and Dnestr river mouths).

Thanks to the changes to the model configuration, the depth of the deep chlorophyll maximum (DCM) is better represented than in previous versions.

Qualitatively, V202211 was the first model version with a sufficiently high vertical resolution to resolve the summer thermocline (around 10-15 m depth) and to sustain a second, shallower deep chlorophyll maximum (DCM). This DCM is distinct from the deeper DCM located around 50-70 m depth (just above the permanent halocline); and is also detected by observations. This change is conserved in V202311. Similar to V202211, V202311 uses near real-time Danube discharge data.

Oxygen: The comparison of model and BGC-ARGO data reveals a bias of 9.28 mmol/m³ and a Pearson correlation coefficient of 0.96. The Nash-Sutcliffe number is in the same class as the previous model versions: "excellent".

Carbonate system: DIC, TA, pH, pCO₂ and CO₂ air-sea flux are compared to climatologic and historical values, and are all within the range of accepted values. The nitracline intensity and depth are improved compared to V202211.

Optics: photosynthetic active radiation (PAR) and attenuation coefficients (Kd) are compared with in situ (BGC-ARGO) and satellite data. The EANs reveal that the normalized PAR is extremely well represented (mostly unchanged from V202211). The comparison of the modelled and observed attenuation coefficient Kd is not straightforward, as detailed in section V; yet the results are very satisfactory when comparing with BGC-ARGO measurements.





Ref: CMEMS-BLK-QUID-007-010
Date: September 2023

Issue: 4.0

II.1 Estimated Accuracy Numbers

Table 1: Selected Estimated Accuracy Numbers (EANs). We use different statistics in order to assess the performances of the model in different aspects (e.g. variability, accuracy).

| Variables | Metrics | Units | Value |
|--------------------------------------|---------------------|----------------------|--------------------------------|
| Oxygen (in situ) | bias | mmol m ⁻³ | 9.28 |
| | RMS | mmol m ⁻³ | 31.75 |
| | Nash-Sutcliffe | / | 0.85 |
| | Pearson correlation | / | 0.96 |
| Oxygen profile maximum (in situ) | bias | mmol m ⁻³ | 52.99 |
| Chlorophyll (satellite) for deep sea | bias | mg/m ³ | 0.007 to 0.017 0.06 to 2.16 |
| for coastal areas | | | 0.00 to 2.10 |
| Depth of maximum | bias | m | 26.3 |
| Chlorophyll (in situ) | RMS | m | 30.4 |
| Normalized | percentage bias | % | -19.86 |
| Photosynthetic Active Light (PAR) | standard dev. ratio | / | 1.14 |
| Light (1711t) | Nash_Sutcliffe | / | 0.80 |
| | Pearson correlation | / | 0.90 |





Ref: CMEMS-BLK-QUID-007-010

Date: September 2023

Issue: 4.

III PRODUCTION SYSTEM DESCRIPTION

III.1 Production centre details

a) Production centre name: BLK-MFC

b) Production subsystem name: BLK-MFC-Biogeochemistry

c) Production Unit: ULiège (MAST)

d) Production centre description for the version covered by this document

The biogeochemical hindcasts and forecasts for the Black Sea are produced by the MAST / ULiège Production Unit by means of the NEMO v4.2 circulation model online coupled with the BAMHBI biogeochemical model, and the "Ocean Assimilation Kit" (OAK) data assimilation framework. The nominal production runs at the Cenaero (Belgium) Tier-1 supercomputing centre called Zenobe, and the backup production runs at the ULiège/CECI "nic5" supercomputing facility.

III.2 Description of the production system

Description of the Black Sea BIO operational system.

The Black Sea biogeochemical model (BLK-Biogeochemistry) is the Biogeochemical Model for Hypoxic and Benthic Influenced areas (BAMHBI, Gregoire et al., 2008; Grégoire and Soetaert, 2010; Capet et al., 2016). It describes the food web from bacteria to gelatinous carnivores through 24 state variables including three groups of phytoplankton: diatoms, small phototrophic flagellates and dinoflagellates, two zooplankton groups: micro- and mesozooplankton, two groups of gelatinous zooplankton: the omnivorous and carnivorous forms, an explicit representation of the bacterial loop: bacteria, labile and semi-labile dissolved organic matter, particulate organic matter. The model simulates oxygen, nitrogen, silicate and carbon cycling. In addition, an innovation of this model is that it explicitly represents processes in the anoxic layer.

Biogeochemical processes in anaerobic conditions have been represented using an approach similar to that used in the modelling of diagenetic processes in the sediments lumping together all the reduced substances in one state variable. In this way, processes in the upper oxygenated layer are fully coupled with anaerobic processes in the deep waters, allowing performing long term simulations. This full coupling between aerobic, suboxic and anoxic processes is absolutely necessary for performing the longterm reanalysis. Processes typical of low oxygen environments like denitrification, anaerobic ammonium oxidation (ANAMMOX), reduced decomposition efficiency have been explicitly represented (Gregoire et al., 2008). Moreover, the model includes a representation of diagenetic processes (Capet et al., 2016) using an efficient and economic representation as proposed by Soetaert et al. (2000). The incorporation of a benthic module allows to represent the impact of sediment processes on important biogeochemical processes such as sediment oxygen consumption (that is responsible for the generation of hypoxic conditions in summer), the active degradation of organic matter that determines the vigour of the shelf ecosystem (~30 % of the primary production produced in shelf waters is degraded in the sediment) and the intense consumption of nitrate by benthic denitrification that filters a substantial part (~50 %) of the nitrogen brought by the north-western shelf rivers (the Danube being the most important one) and modulates primary production in the deep basin. In addition to a representation of diagenesis, the biogeochemical model represents the transport of sediments by waves. This is an important feature that is necessary in order to sustain the primary production of the deep basin.





Ref: CMEMS-BLK-QUID-007-010
Date: September 2023

Issue: 4.0

Since V201907, BAMHBI has been extended with a module describing the carbonate dynamics. As in Soetaert et al. (2007), the model solve for DIC and the Excess Negative charge from which is computed TA (considering the contribution of sulphide), pH, the speciation of DIC ([HCO_3]⁻, [CO_3]⁻, [CO_3], and CO_2 aircsea flux

Since V202007, the forecasting system includes data assimilation of daily level-3 satellite observations of surface chlorophyll.

At V202211, the chlorophyll content of each phytoplankton group is a model state variable (Geider et al, 1998).





Ref: CMEMS-BLK-QUID-007-010

Date: September 2023 Issue: 4.0

Description of the Production chain

The V202311 version of the model is a major upgrade of the modelling system with the following changes: (1) a new version of the physical model, i.e. NEMO 4.2.0. instead of NEMO 4.0.6., (2) the vertical discretisation is improved, leading to a better representation of processes around the deep chlorophyll maximum, the nitracline, the oxycline, the halocline and the cold intermediate layer, (3) different physical, biogeochemical and data assimilation parameterizations are better tuned 4) an explicit modelling of the chlorophyll content of each plankton functional type.

At V202311, the BS-Biogeochemistry model is online-coupled with the NEMO v4.2 ocean model and is run with a horizontal resolution of ~2.5 km and 59 vertical levels using z-layer vertical coordinates. This NEMO configuration has fine-tuned physical processes that are known critical for simulating Black Sea biogeochemistry. This includes the open boundary condition at the Bosporus (based on Stanev et al, 1997; Stanev and Beckers, 1999), a new package to ensure strict conservation of the biogeochemical tracer budgets, the GLS turbulent closure scheme and a refined light penetration scheme. There is currently no feedback from the biology to the light absorption in the physical model. BS-BIO NRT system runs each day one day of analysis and 10 days of forecasts.

Once per week (on Tuesdays), a 10-day analysis is performed during which the model assimilates daily L3 satellite chlorophyll observations. Chlorophyll content of the 3 phytoplankton groups is updated; but the assimilation increment is also back-propagated to the carbon-content and nitrogen-content of the phytoplankton groups before the model is restarted. The 3 phytoplankton groups are modified together, i.e. the ratios between them remain unchanged by the assimilation procedure. Similarly, the ratio between chlorophyll, carbon and nitrogen in each phytoplankton group is not modified.

The assimilation increments are 3D, i.e. the analysis modifies the model variables also below the surface layer. The modification in depth is limited to the extent of the mixed layer.

The V202211 model was initialized on 01/01/2021 (from the V202211 simulation).

Commented [GM3]: Je voulais enlever forcing car il me semblait que l'on utilisait forcing surtout lorsqu'il n'y avait pas de feedback?

Commented [VL4]: ok

Commented [GM5]: Correct?

Commented [VL6]: oui c'est correct

Commented [GM7]: C'est évidemment une hypothèse qui

Commented [VL8]: oui... Geider fonctionne bien, mais je pense qu'il y a trop de chloro sur le shelf en été (probablement due à de l'eau turbide?) --> il y a encore du travail pour bien tuner tout le modele avec Geider





Ref: CMEMS-BLK-QUID-007-010

Date: September 2023

Issue: 4.

III.3 Upstream data and boundary condition of the NEMO-BAMHBI model

The CMEMS-BS-MFC-Biogeochemistry analysis and forecast system uses the following upstream data:

- 1. Atmospheric files of air temperature, air dew temperature, total precipitation, cloud coverage, wind velocity and mean sea level pressure produced by ECMWF analysis and forecast fields (i.e. at $1/8^{\circ}$ spatial resolution with 3hr and 6hr temporal resolution) are used to force NEMO physics and for the wind, to compute the air-sea exchanges of O_2 and CO_2 .
- 2. Atmospheric deposition of inorganic nitrogen delivered by Kanakidou et al. (2012) that have a similar order of magnitude than river inputs and are needed to sustain primary production in the deep basin.
- 3. The data assimilation scheme uses the daily L3 CMEMS Ocean-Colour satellite observations (product OCEANCOLOUR BS CHL L3 NRT OBSERVATIONS 009 044).
- 4. The BS-BIO NRT system uses near real-time freshwater discharge data from the Romanian Hydrological Institute for the Danube, by far the most important river in the Black Sea. The data is provided for the 3 main arms of the river. The nutrient load concentration however, is climatological. For the other rivers (Dniepr, Dniestr, Rioni, Sakarya and Kizilirmak), due to the absence of NRT data, the BS-BIO NRT system uses climatological values of river flows, inorganic nutrients and organic materials inputs computed from the long time series of data provided by Ludwig et al., (2009) in the frame of the EU SESAME and PERSEUS projects.
- 5. The Bosporus Strait is considered as an open boundary as in Stanev et al, 1997; Stanev and Beckers, 1999. The velocity and salinity are determined in such a way that total seawater and salt are conserved in the Black Sea domain. Temperature use a zero-gradient boundary condition. Biogeochemical variables use zero-gradient ("Neumann") or fixed value ("specified") boundary conditions.





Ref: CMEMS-BLK-QUID-007-010

Date: September 2023

Issue: 4.0

IV VALIDATION FRAMEWORK

The quality assessment of the V202211 analysis-forecast BS-MFC-Biogeochemistry system (described in the previous section) has been done by comparing a simulation that covers the period 2020-2021 with available NRT observations, similar to what has been done for previous versions. The product quality activities used both quantitative metrics and qualitative assessment approaches. The metrics used for the quantitative validation are reported in **Table 2**. These error statistics are computed for oxygen and chlorophyll for which we have NRT data thanks to satellite and BGC-ARGO. Some variables could not be validated in NRT, such as nutrients (nitrate and phosphate), phytoplankton biomass, primary production, carbonate system due to the lack of NRT data for such variables. These variables are however validated for the reanalysis (see CMEMS-BS-QUID-007-005) and as concern the carbonate variables, they have been compared with historical data that have been considered of high enough quality (e.g. Sesame, KNORR). We also compare the density profiles of inorganic variables (e.g. NO₃, O₂, DIC, Alkalinity, pH, ODU, NH₄, PO₄, SiO₂) with data aggregated profiles found in the literature.

NRT Datasets

The datasets used to validate the product are the following:

- In situ ARGO observations are downloaded from the CMEMS in-situ TAC (product: INSITU_BS_NRT_OBSERVATIONS_013_034); they can also be obtained from the Coriolis (Brest, France) website, see http://www.coriolis.eu.org/. They are used for the validation of physical variables (temperature, salinity, and derived quantities such as mixed layer depth (MLD), Cold Intermediate Water (CIL) Cold Content (CCC)) and biogeochemical variables (oxygen, chlorophyll, light).
 - For chlorophyll provided from BGC Argo fluorescence measurements, a correction is used, adapted for the Black Sea (high content of CDOM, anoxia) as described in Ricour et al. (2021).
- 2) BLKSEA_ANALYSIS_FORECAST_BIO_007_010 V202105 (the previous versions of this product)
- 3) CMEMS OC-TAC satellite Level-3 observations for the Black Sea were obtained from CMEMS (product OCEANCOLOUR_BS_CHL_L3_NRT_OBSERVATIONS_009_044).

Error Metrics

The quality assessment of model results is done using different errors statistics that allow to quantify model-data mismatches on different aspects. **Table 2** presents these statistics (more details can be found in Allen et al., 2007). For the definition of the metrics, "O" represents the observations and "P" is the model output. In addition to these global statistics we assess the ability of the model to simulate the monthly vertical profiles of oxygen and its maximum value.

For chlorophyll, the model – observation comparison has been performed by splitting the basin in 11 sub-regions as done by Kopelevich et al. (2003). This partitioning is essentially based on the depth: regions shallower than 50 m, between 50 and 200 m, and deeper than 200 m. Furthermore, these regions are divided in eastern / western zones. The obtained map of regions is shown in **Figure 1**, white dots indicate the location of in situ BG-ARGO measurements.





Ref: CMEMS-BLK-QUID-007-010

Date: September 2023

 Table 2: List of metrics -- used to assess the model performance.

| Definition | Meaning | Interpretation |
|--|--|---|
| The percentage bias (no units) $PB = \frac{P - O}{O} * 100$ | Compares the mean values of <i>O</i> and <i>P</i> , and expresses the average bias as a percentage value of the <i>O</i> average | PB>0: global overestimation PB<0: global underestimation PB <10%: excellent skill, 10-20: very good, 20-40: good, > 40 poor (Maréchal, 2004) |
| Standard deviation ratio (no units) $r_{\sigma} = \frac{\sigma_{O}}{\sigma_{P}}$ | Compares the distribution of <i>O</i> and <i>P</i> around their respective average | >1: larger variability in the observations <1: larger variability in the model |
| Nash-Sutcliffe efficiency (no units) $N - S = 1 - \frac{\sum (O - P)^2}{\sum (O - O)^2}$ | Relates the model errors to the variability in the observations. | >0.65: excellent >0.5: very good >0.2: good <0.2: poor (Maréchal, 2004) |
| Pearson correlation coefficient (no units) $ ho$ | Indicates how the variations of O and P around their respective mean are related | Significant correlations can be concluded for values of ρ above threshold values according to the amount of available data |
| Chi-squared statistic (no units) $\chi^2 = \frac{1}{n \sigma_o^2} \sum (P - O)^2$ | Is an estimation of the model cost | The lowest χ^2 , the better. This statistic is useful for comparing different versions of the model (model evolution) |





Ref: CMEMS-BLK-QUID-007-010
Date: September 2023

Issue: 4.0

Commented [rvw9]: Inserted it in a table so that it doesnt move.

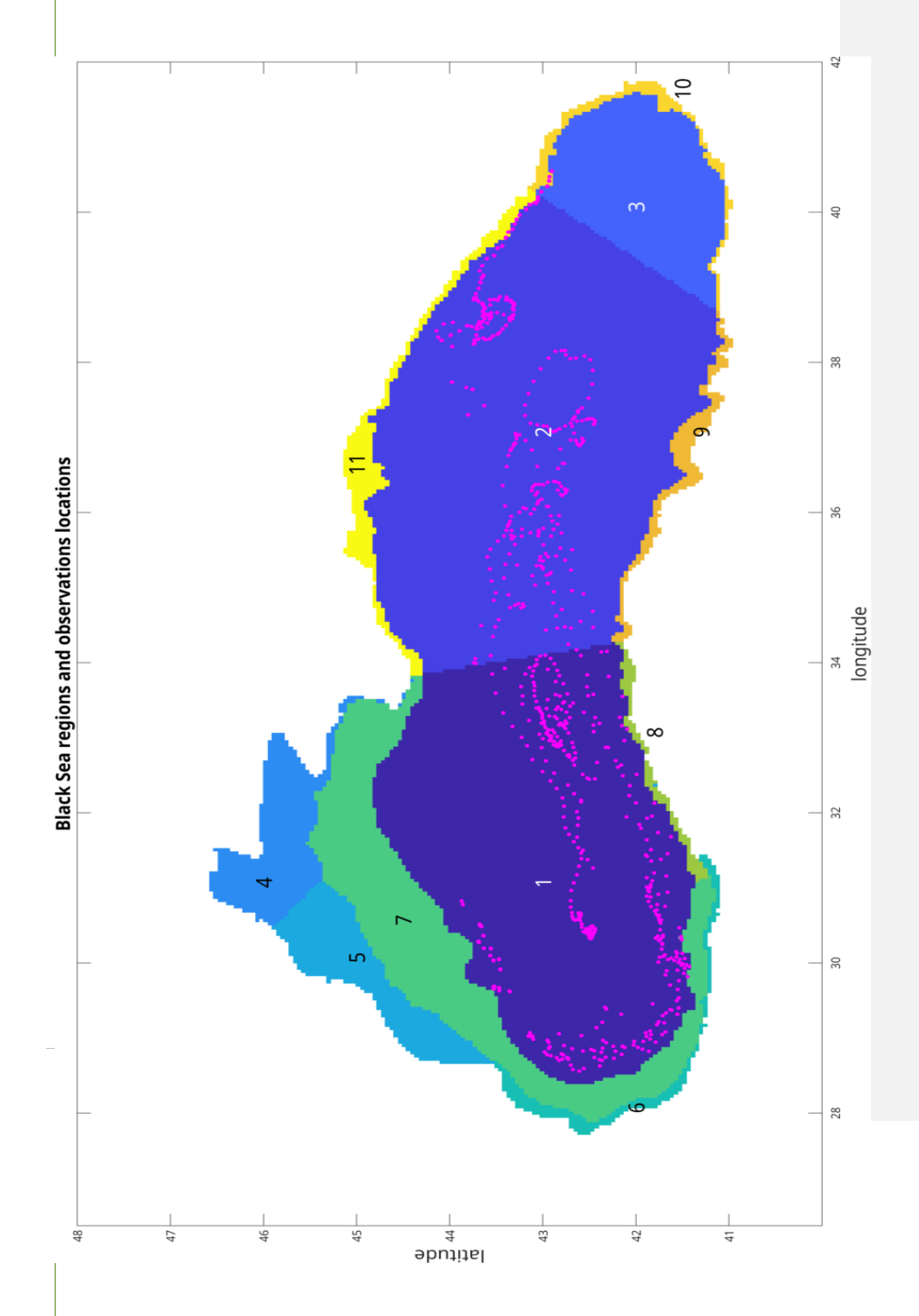




Ref: Date:

CMEMS-BLK-QUID-007-010

e: September 2023



Ref: CMEMS-BLK-QUID-007-010
Date: September 2023

Issue: 4.0

Figure 1: Sub-Regions (based on Kopelevich et al., 2003) used for computing the error statistics for chlorophyll. The numbers indicate the regions of the Black Sea. Regions 1-3 are the "open sea", regions 4-5 is the North-Western Shelf and region 7 is a transition region. The dots represent the position of the observed profiles





Ref: CMEMS-BLK-QUID-007-010

Date: September 2023

Issue: 4.

V VALIDATION RESULTS

In the following we first analyze the performances of the BLKSEA_ANALYSIS_FORECAST_BIO_007_010 product at the V202311 release, focusing on physical variables that are known to act as primary controls on biogeochemistry (e.g. mixed layer depth, ventilation).Next, for biogeochemical variables we will mainly focus on the validation of oxygen, chlorophyll, PAR and Kd because they are the only variables available in NRT. For oxygen, we will assess the global statistics of the model (computed over the whole model domain and period of simulations), its ability to represent the monthly oxygen vertical profiles and value of the maximum concentration. For chlorophyll, we will compare model results with satellite product for the different regions identified in **Figure 1**; we will also compare with the chlorophyll retrieved from fluorescence data provided by BGC-ARGO. Finally, we qualitatively compare the carbonate system to climatology.

V.1 Physical variables

The Black Sea presents an oxygen-rich surface layer on top of an anoxic water mass. Basin ventilation is mainly governed by the formation each year of cold oxygen-rich waters that accumulate at depth to form the Black Sea Cold Intermediate Layer (CIL). The ventilation mechanism is limited by a permanent halocline. In this section, we assess the capacity of the BS-BIO physical model (NEMO 4.2) to simulate the formation of the CIL and mixing processes by comparison with observations.

V.1.1 Mixed Layer Depth (MLD)

In the Black Sea, the general criterion for the MLD is usually a density gradient above 0.125 kg m 3 referenced at 3 m (Kara et al., 2009). However, the use of the definition is compromised by the lack of high-quality data close to the surface (<10 m depth). Hence, the model MLD is computed at each point as the depth where the density is 0.125 kg/m 3 larger than the density at 10 m depth, and then spatially averaged over the basin. The basin averaged model MLD (for points where the depth is at least 50 m) is compared with punctual Argo derived MLD. Results over 2021-2023 are shown in **Figure 2**.

The model is able to reproduce the typical seasonal MLD cycle (**Figure 2**). During the winter, spring and summer, NEMO simulates an averaged MLD inside the range of ARGO values. During the autumn, the simulated MLD is in the upper range of ARGO estimates.

The NEMO configuration update from V202105 to V202211 includes a change in vertical resolution; the upper layers are much smaller in the new version. As will be explained later, this allows a better representation of the shallow summer thermocline (not shown here). This change cannot be represented here as by construction, the MLD estimate cannot be shallower than 10 m (either for the model or the ARGO observations).





Ref: CMEMS-BLK-QUID-007-010
Date: September 2023

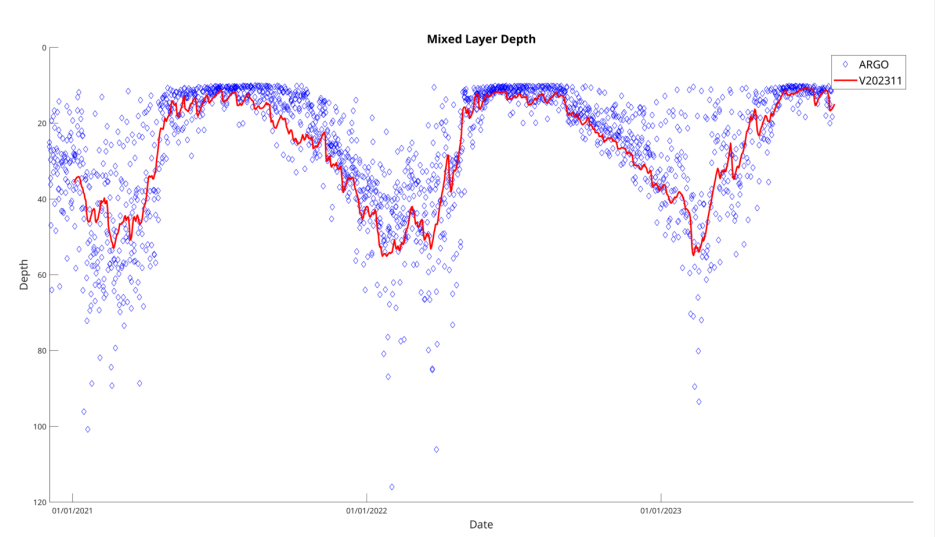


Figure 2. Mixed layer depth in red (spatial average over the points where the bathymetry is larger than 50 m) computed from V202311 (NEMO 4.2.0), and in blue from T,S profiles from ARGO floats.





Ref: CMEMS-BLK-QUID-007-010

Date: September 2023 Issue: 4.0

V.1.2 Cold Intermediate Layer

The Black Sea Cold Intermediate Layer (CIL) is characterized by temperature lower than 8.35°C, and density larger than 1014 kg m⁻³. This water mass is abundantly described in the literature. The amount of CIL, called "CIL Cold Content" (CCC) can be estimated from temperature and density values as the deficit of heat in the CIL compared to a 8.35°C-layer. **Figure 3** shows the CCC estimated by the NEMO model at V202105 and V202211. The agreement between models and observations has been shown in the literature, and in previous versions of this QUID.

Switching to V202311, the CCC created during the winters of 2021 and 2022 is respectively somewhat smaller and larger than for V202211. The change between V202211 and V202311 is due to the different behaviour when using a different vertical discretisation, different vertical and horizontal diffusion, and different parameterization of the heat exchange at the sea surface.

All the versions of the systems show that the CCC is smaller during the last decade compared to previous decades. Furthermore, during the last decade, the CIL is destroyed quickly, and in particular, the CIL created during the winters 2021 and 2023 has already disappeared completely in spring.

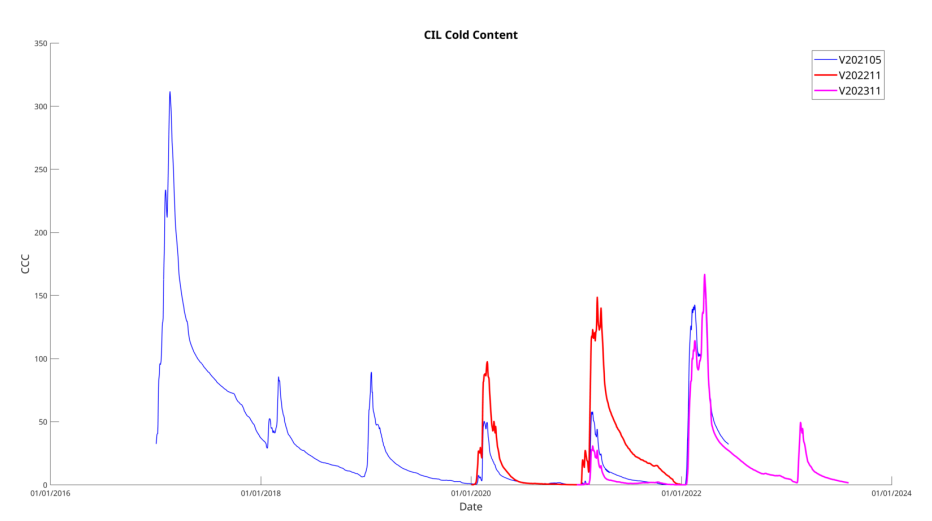


Figure 3. CCC from V202105, V202211 and V202311.





CMEMS-BLK-QUID-007-010 Ref: Date: September 2023

Issue:

4.0

V.2 Oxygen

The Black Sea's oxycline had shoaled during the recent years (Capet et al., 2016). Although the model simulates this shoaling (see also the QUID for the corresponding multi-year product BLKSEA_MULTIYEAR_BGC_007-005), the model underestimates the velocity of change. In the version V202205 of the system, the simulated oxycline was deeper than that obtained from ARGOs and the oxygen penetration depth is too deep (Table 3). At V202311, the oxycline depth in the model is much closer to the ARGO observations, although a bias still persists, the model oxycline being slightly too deep especially during summer. All EANs are largely improved compared to V202211 (and previous versions), (see Table 3).

Table 3: Model skill statistics obtained for all model-observation predictions pairs for oxygen, with respect to BGC-ARGO observations (see the position of the sites in Figure 1). Error metrics are defined in Table

| Oxygen | Value at V202205 | Value at V202311 |
|------------------------------------|---------------------|------------------|
| Bias (mmol m ⁻³) | 28.5 | 9.28 |
| Rms (mmol m ⁻³) | 59.5 | 31.75 |
| Standard deviation ratio (no unit) | 0.76 | 0.82 |
| Nash-Sutcliffe (no unit) | 0.49 | 0.85 |
| Pearson coefficient (no unit) | 0.89 | 0.96 |

During Jan-2021 - Jul-2023, there were 212 BG-ARGO profiles with oxygen data (all of them are in the deep sea); there were at least 15 profiles every month (over the combined years in the period 01/2021-07/2023). Figure 4 compares all the modelled and BGC-ARGO oxygen profiles, arranged by month.

Commented [GM10]: Un lien?

Commented [VL11]: il va changer, mais j'ai mis plus



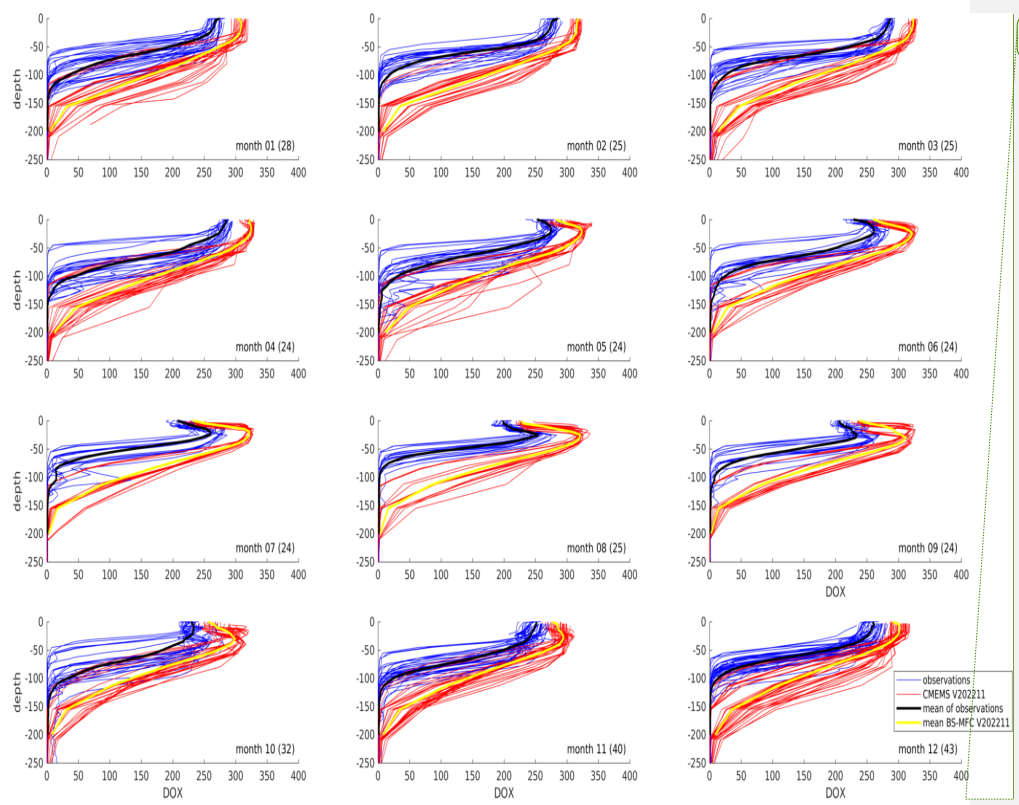


Ref: Date:

CMEMS-BLK-QUID-007-010

: September 2023

Issue: 4.0



Commented [rvw12]: Made this figure bigger to make text more readable.





Ref: Date: CMEMS-BLK-QUID-007-010

September 2023

Issue: 4.0

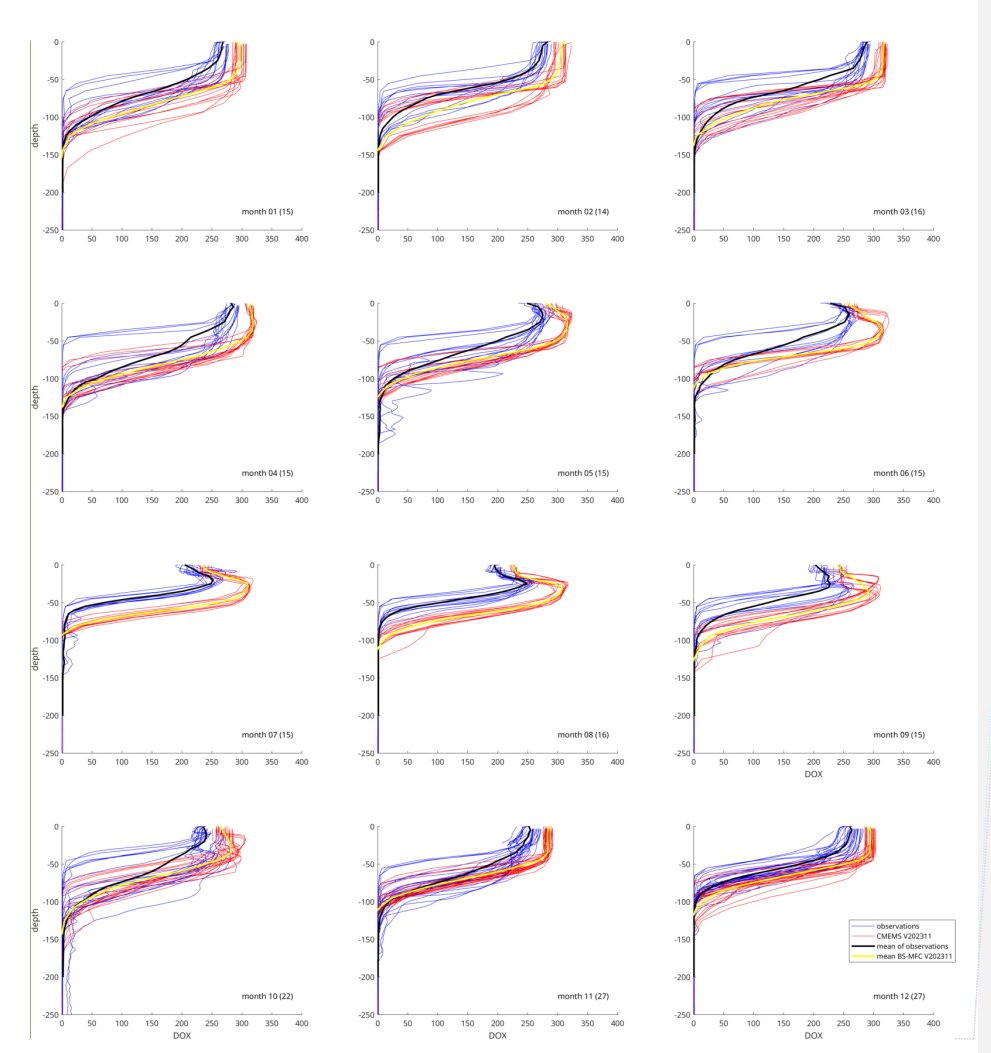


Figure 4: Oxygen profiles for each month during Jan-2021- Jul/2023 (model in red, in situ observations in blue; the model and observed monthly mean profiles are respectively in yellow and black)

Similar to previous versions, the oxygen maximum is well simulated by the model, with a mean bias of 52.99 mmol.m⁻³, corresponding to a percentage bias of 20.4 %. As an example, the complete time-series of oxygen measurements by BGC-Argo buoy 6903240, and its model equivalent, are shown in Figure 5.

COPERNICUS MARINE ENVIRONMENT MONITORING SERVICE

(opernicus



Commented [GM13]: On voit clairement dans les Argos un resserrement de l'oxycline en juin et juillet. Je ne sais pas si cela se voit dans la physique aussi. Si c'est du à un chgm saisonnier ou à une variabilité spatiale de la bouée.

En hiver le modèle oxygénise de trop la surface. Cela doit être du à des températures trop basses dans le modèle. Possible? Il faudrait regarder T et S aux mêmes endroits.

Tu ne montres pas 2021-2022?

Commented [VL14]: d'accord pour les conclusions de la physique (tempature) sur l'oxygene

Commented [VL15]: je me suis trompé dans la légende, c'est

Ref: CMEMS-BLK-QUID-007-010
Date: September 2023





Ref: CMEMS-BLK-QUID-007-010
Date: September 2023

Issue: 4.0

Dissolved Oxygen

For next versions, please make sure the text in plots can be read.

101-Apr-2021 01-Jul-2021 01-Jul-2022 01-Apr-2022 01-Jul-2022 01-Dc-202 01-Dc-202

Figure 5. Model-observation comparison for oxygen: Above: Hovmoller diagram for BGC-ARGO buoy 6903240 up to its end-of-life. Below: model equivalent.





Ref: Date: CMEMS-BLK-QUID-007-010

September 2023

Issue: 4.0

V.3 Chlorophyll

In this section, chlorophyll concentration obtained from the model, from satellite L3 chlorophyll concentration, and from ARGO floats are compared for the period 01/2021-07/2023.

Two major changes from V202005 to V202211 concerned the model's vertical resolution and the use of near real-time Danube discharge water. As mentioned before, the increased vertical resolution allowed, for the first time, to represent the shallow summer thermocline, which can then sustain the shallower deep chlorophyll maximum (DCM).

It was shown during the switch to V202211 that the use of a higher vertical resolution has allowed to represent the shallow summer thermocline, sustaining a second deep chlorophyll maximum. Furthermore, the use of near-time freshwater discharge data for the Danube allows to improve the chlorophyll concentration, e.g. it allowed to represent a late-summer / autumn bloom previously missing. Figure 6 shows the time-series of surface chlorophyll concentration during the V202211 spin-up year (2019) realized without data assimilation, for both cases of climatological Danube data and the near real-time Danube Data. The time-series is plotted for a point offshore of the Danube River mouths (250 km away from the Saint-George mouth of the Danube). If the spring bloom is very similar for both cases, the near real-time discharge data brings an autumn bloom missing in the simulation with climatological discharge data.

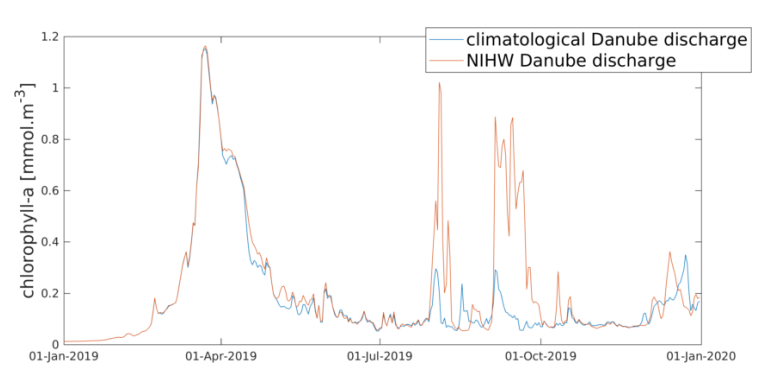


Figure 6: Time-series of surface chlorophyll during a simulation without data assimilation, for climatological and near-real time Danube river discharge data

These modifications (i.e. additional blooms due peak discharges)- are still present in V202311.

V.3.1 Satellite data

The regional time-series are computed by averaging, every day, all available points in each sub-region shown in **Figure 1**. For satellite products, if the level-3 (L3) image over a particular region presents many clouds and does not have at least 100 pixels, the result for that day and region is not computed and the time-series presents a gap.

The satellite observations used in the comparison are taken from the CMEMS MY reprocessed L3 images





Commented [GM17]: C'est étonnant que le DCM soit au dessus de la thermocline. D'abbitude c'est en dessous ou dans la thermocline afin de profiter des nutriemnts qui sont juste en dessous. A moins qu tu aies les nutriments en surface apportés par les apports atm?

Commented [VL18]: en faut je ne sais pas si c'est au-dessus ou dedans ou-dessous (je n'ai pas checké)... mea culpa

Commented [VL19]: la seule chose dont je suis sur, c'est quil y a (parfois) un DCM vers la hauteur de la thermocline en question, ce qui n'etait (logiquement) jamais le cas avec 31 niveaux

Ref: CMEMS-BLK-QUID-007-010 Date: September 2023

Issue: 4.0

(CMEMS product 009_153, REProcessed product based on multi-satellite composites). They are obtained by an algorithm combining results from a neural network (in the coastal areas) and a classical ratio-based method (in the open sea).

The time-series shown in the left column of **Figure 7** concern the first 3 regions in the open sea. Compared to older model versions, the V201907 model and satellite values were in much better agreement. At V202007 and V202211, in the open sea, the assimilation of satellite chlorophyll observations brought the model even (much) closer to the observed values. At V202311, the chlorophyll content of phytoplankton groups is a model state variable (rather than a diagnostic variable computed from the carbon and nitrogen contents). In the open sea, the model bias with respect to satellite estimates is even smaller than at V202211, respectively 0.0172, -0.0108 and 0.0068 mg.m⁻³ in the western, central and eastern basin. The root mean square error is unchanged at 0.1 mg.m⁻³, The standard deviation ratio is between 0.99 and 1.18, indicating that the model has a slightly larger standard deviation than the satellite estimates. Pearson correlation coefficients are between 0.67 and 0.76 (slightly smaller than at V202211); the Nash-Sutcliffe coefficient is "excellent" as at V202211.

The panels in the right column of **Figure 7** shows the time-series in the NWS regions. Region 4 is influenced by the Dnestr and Dnepr, whereas region 5 is directly in front of the Danube. Hence, for these regions, the river discharge (flow) as well as river water nutrient concentration are critical. Since version V202211, for the Danube river the freshwater flow is obtained in near-real time from a hydrological model; whereas for the other rivers, it is obtained from monthly climatology. The nutrient discharge values are climatological values for all the rivers. In these regions, some differences between model and observations persist even after the assimilation of the satellite chlorophyll. The bias is positive: 2.15 and 0.88 mg.m⁻³ in regions 4 and 5 respectively.

Region 6 is also a shelf region, located to the South of the NWS, and is less sensitive to rivers (bias=0.10 mg m $^{-3}$). Region 7 is the transition region between the NWS and the open sea, and here also, the model and observations are very close (bias = 0.06 mg m $^{-3}$).





Ref: Date: CMEMS-BLK-QUID-007-010

September 2023

Issue: 4.0

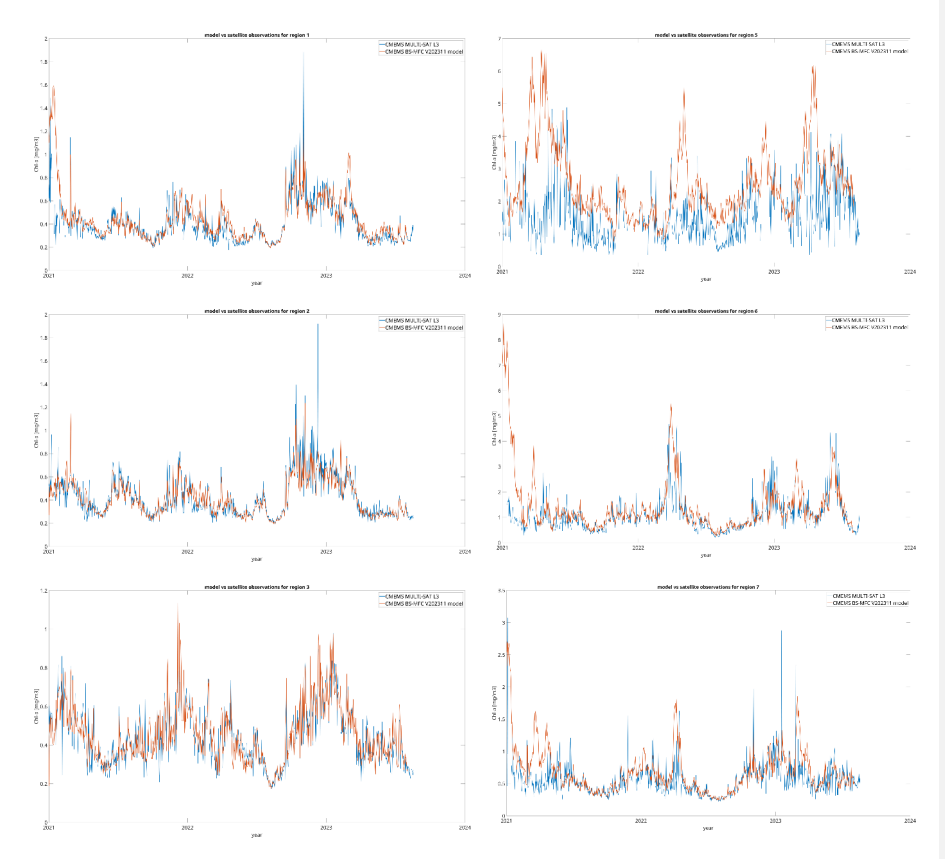


Figure 7: Time series of satellite (in blue) and model (in red) chlorophyll spatial averages computed for (left column) open sea sub-regions 1, 2 and 3, and (right column) NWS regions 5, 6 and 7. The regions are shown in Figure 1.

Table 4 shows the bias between the model and observations, expressed in mg. m^{-3} . Compared to V202105, the error statistics indicate a similar very low bias, which is clearly a consequence of data assimilation.

Table 4: bias statistic for chlorophyll obtained for V202311 when considering the observation-model prediction pairs, for the different regions (1 to 11). The bias error metric has been defined in **Table 2**. Data are the multi-year (MY and MYinterim) CMEMS satellite observations.

| AEN /Region | 1 | 2 | 3 | 4 | 5 | 6 | 7 | 8 | 9 | 10 | 11 |
|-------------|--------|--------|-------|------|------|-------|-------|-------|-------|-------|--------|
| Bias | 0.0172 | -0.011 | 0.007 | 2.16 | 0.88 | 0.103 | 0.061 | 0.228 | 0.056 | 0.142 | -0.056 |





Ref: CMEMS-BLK-QUID-007-010
Date: September 2023

Issue: 4.

V.3.2 In situ data

At the beginning of 2021, there were 2 BGC-ARGO in the Black Sea that collect oxygen and chlorophyll, all of them being in the central basin and never on the North-Western shelf. From October 2021, 2 supplementary floats were deployed and hence there are currently 4 BGC-ARGO floats.

The estimation of the chlorophyll concentration from the fluorescence data provided by the BG-ARGO cannot be made using a generic algorithm. Indeed, due to the presence of anoxic conditions it seems that the chlorophyll pigments are not efficiently degraded, and this makes that fluorescence is increasing with depth in the Black Sea. If generic algorithms are used this means that the chlorophyll concentrations will also increase with depth, reaching approx. 0.3 mg/m⁻³ at 1000 m depth. Therefore, a specific correction (on the model of Xing et al., 2017) was applied to the deep chlorophyll which essentially sets it to zero. The corrected data from BGC-ARGO floats are stored at ULiege (Ricour et al. 2021).

The comparison of the deep chlorophyll maximum (DCM) in the profiles shows that the model somewhat overestimates the DCM strength, with a bias of of 0.34 mg.m⁻³. The variability in the model and observations is similar (standard deviation ratio: 1.02).

The comparison of the depth of the DCM between the *in situ* observations and the model shows that the model chlorophyll maximum is too deep during the summer. The bias is 26.3 m. Error statistics are shown in **Table 5**.

Table 5: Model error statistics obtained when considering model - in situ observations (see the position of the sites in **Figure 1**) pairs for chlorophyll. Error metrics are defined in **Table 2**.

| Intensity of chloophyll maximum | Value at V202311 |
|---------------------------------|------------------|
| Bias (mg.m ⁻³) | 0.33 |
| RMS (mg.m ⁻³) | 1.26 |
| sdr (/) | 1.02 |
| Depth of chlorophyll maximum | Value at V202311 |
| Bias (m) | 26.34 |
| RMS (m) | 30.38 |
| sdr (/) | 0.99 |





| QUID for BLK MFC Products | | | | | | | |
|-----------------------------------|----|--|--|--|--|--|--|
| BLKSEA_ANALYSISFORECAST_BGC_007_0 | 10 | | | | | | |

Ref: CMEMS-BLK-QUID-007-010 Date: September 2023

Issue: 4.0

V.4 Carbonate sub-system

The validation of the carbonate system is not possible in NRT. Besides, even for the past the quality of carbonate data (e.g. pH) is sometimes not optimal. Also, for assessing the consistency of the simulated carbonate components, we used KNORR 88 observations described in Goyet et al. (1990), Knorr (2001) data and Sesame 2008 data (Borges, personal communication). In addition, we compared with typical profiles collected on a density scale and presented in Moiseenko et al. (2011). When comparing model values to climatologic measurements, the comparison is best performed as a function of the density anomaly, σ_t [kg.m⁻³], instead of depth because it is well know that in the Black sea most of biogeochemical variables present particular characteristics at specific density levels. At the surface, σ_t is around 11; it increases to 14-16 in the oxycline zone, and rises up to 16.2 at the starting of the anoxic layer and to 17-17.5 at the bottom.

V.4.1 Oxygen and Nitrate

Figure 8 shows the simulated oxygen on a density scale. Oxygen was already compared to observations in section V.2. The model is able to simulate the disappearance of oxygen at a density of 15.8-16 in agreement with data profiles. In **Figure 9**, the nitracline is clearly visible around σ_t =15.2 kg m⁻³ with a maximum nitrate concentration around 5 mmol.m⁻³ (more in line with recent estimates compared to 4 in V202211). The nitracline vanishes at σ_t =16.0-16.5 kg m⁻³ whereas in V202211 it extended deeper (up to σ_t =17 kg m⁻³). Surface values are highly time- and space-dependent. In particular, on the NWS, very high values can be found close to river mouths (on the NWS shelf, blue points in the plot).

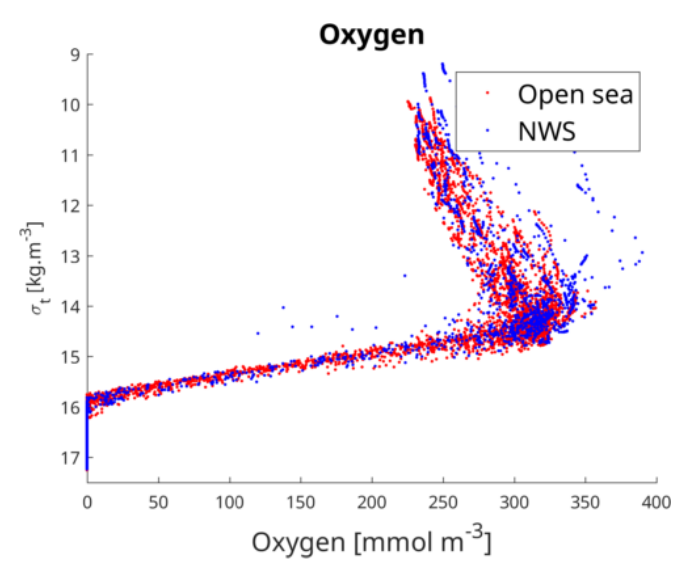


Figure 8: Oxygen as a function of the density anomaly. Vertical profiles are selected randomly in space, and throughout the simulation period (2023-2023), from V202311 model results





Ref: Date:

CMEMS-BLK-QUID-007-010

September 2023

Issue: 4.0

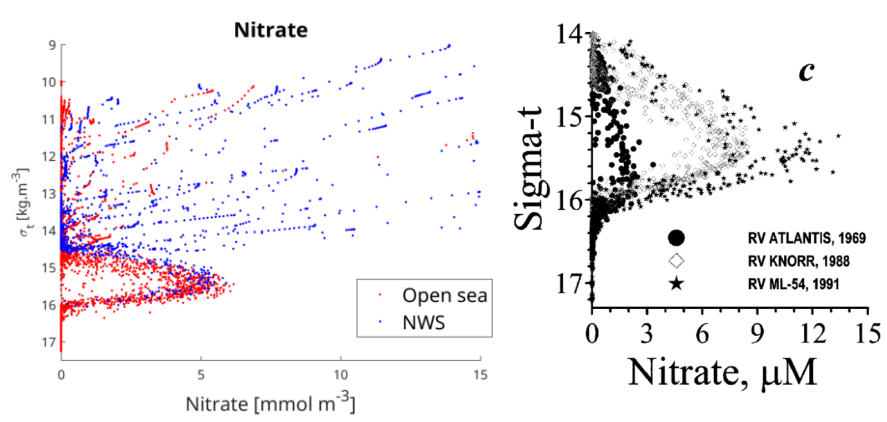


Figure 9: Nitrate as a function of the density anomaly. Left panel: CMEMS BS-MFC V202311 model (2021-2023). Right panel: reprinted from Konovalov and Murray, 2001. It should be noted that compared to the eutrophication period 1988-1992, it is acknowledged that the value of the nitrate peak has decreased to ~4-6 μM (Borges, 2008, unpublished Sesame data in the deep basin) which is in perfect agreement with the order of magnitude simulated by the model.

V.4.2 Dissolved Inorganic Carbon

For the considered period (2021-2023), there are no available measurements of Dissolved Inorganic Carbon (DIC), pH, Total Alkalinity, surface pC02 and air-sea CO2 flux. However, the literature presents some estimates and it is possible to qualitatively check if the modeled values are in the correct range, as a function of density. Results are presented for the different variables in Figure 10 to Figure 13.

Concerning DIC, it can be seen that the modelled values and the ones from the literature indeed correspond very well (Figure 10).

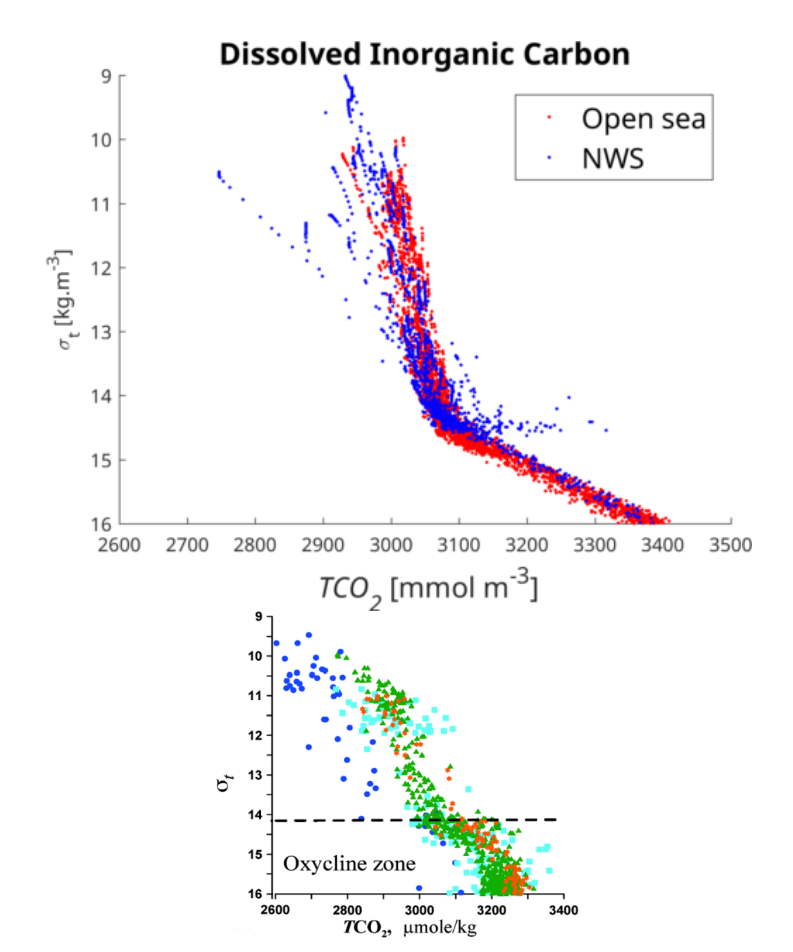




Ref: Date: CMEMS-BLK-QUID-007-010

ite: September 2023

Issue: 4





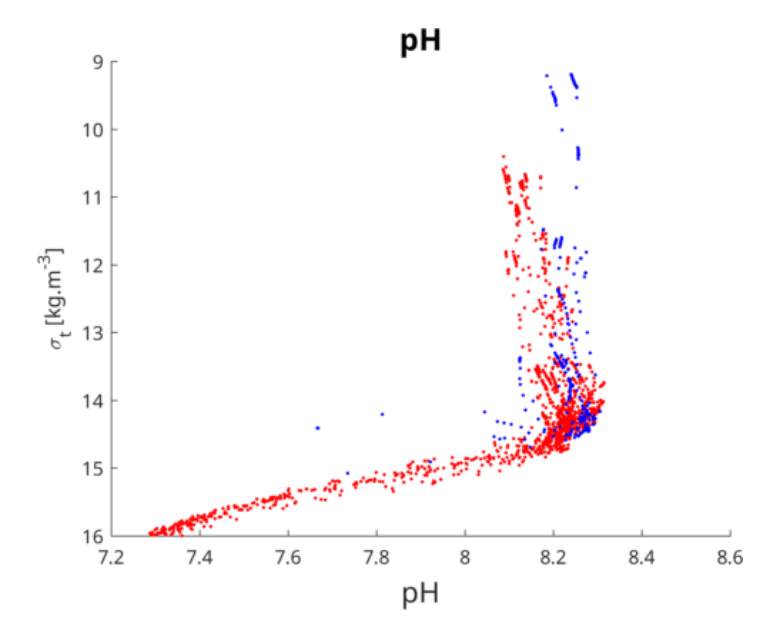


Ref: CMEMS-BLK-QUID-007-010
Date: September 2023

Issue: 4

V.4.3 Figure 10: Dissolved Inorganic Carbon as a function of the density anomaly. Left panel: CMEMS BS-MFC V202311 model (2021-2023). Right panel: reprinted from Moiseenko et al, 2011.pH and Total Alkalinity

As for DIC, values for pH and alkalinity, from the model and from the literature, are compared qualitatively. **Figure 11** shows that the shape of the profiles in function of density, as well as magnitudes of the variables, correspond very well.







Ref:

CMEMS-BLK-QUID-007-010

Date: September 2023

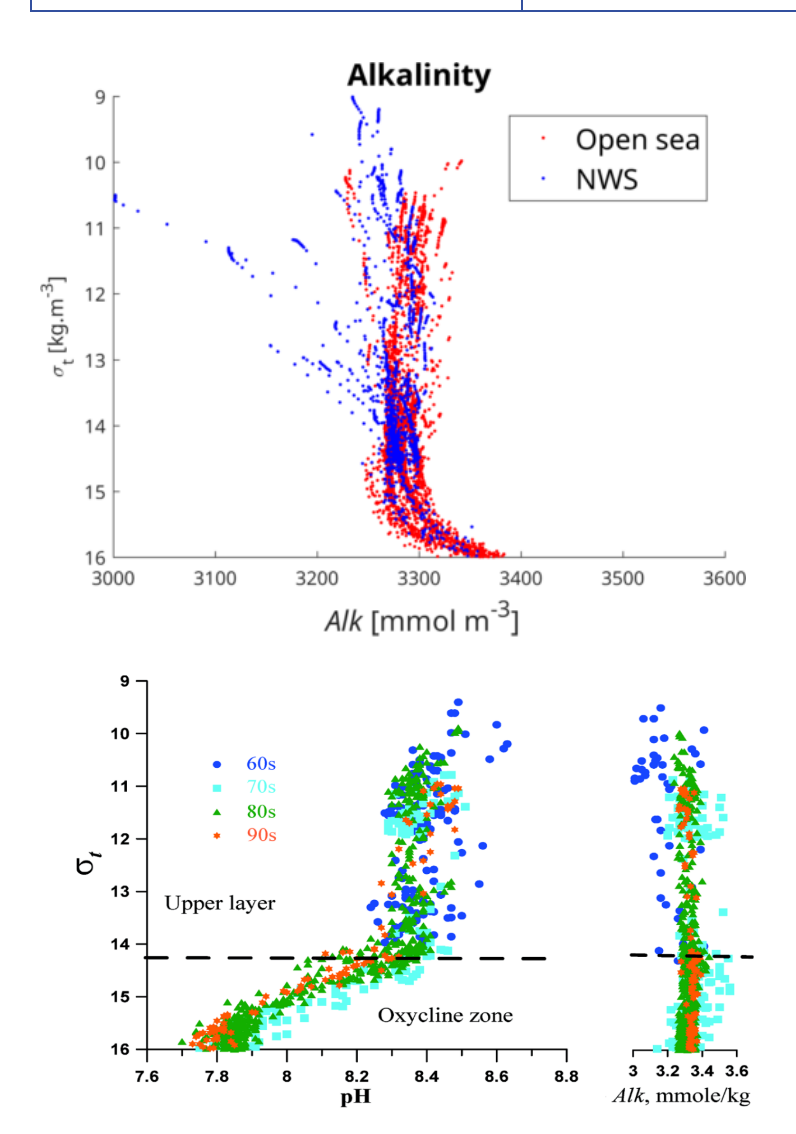


Figure 11: Comparison of model and observations of pH (left) and Alkalinity (right) as a function of the density anomaly. Top panels: CMEMS BS-MFC V202311 model (2021-2023). Lower panels: reprinted from Moiseenko et al. (2011).





| QUID for BLK MFC Pr | oduct | ts | |
|-------------------------|-------|-----|-----|
| BLKSEA_ANALYSISFORECAST | BGC | 007 | 010 |

CMEMS-BLK-QUID-007-010 Ref: Date: September 2023

Issue:

4.0

V.4.4 pC02

For the pCO2 variable, one can again see qualitatively from Figure 12 that model and literature are in good agreement. The right panel shows a tendency of increasing values during the recent decades, and the modeled values (left panel) is indeed in the upper range.

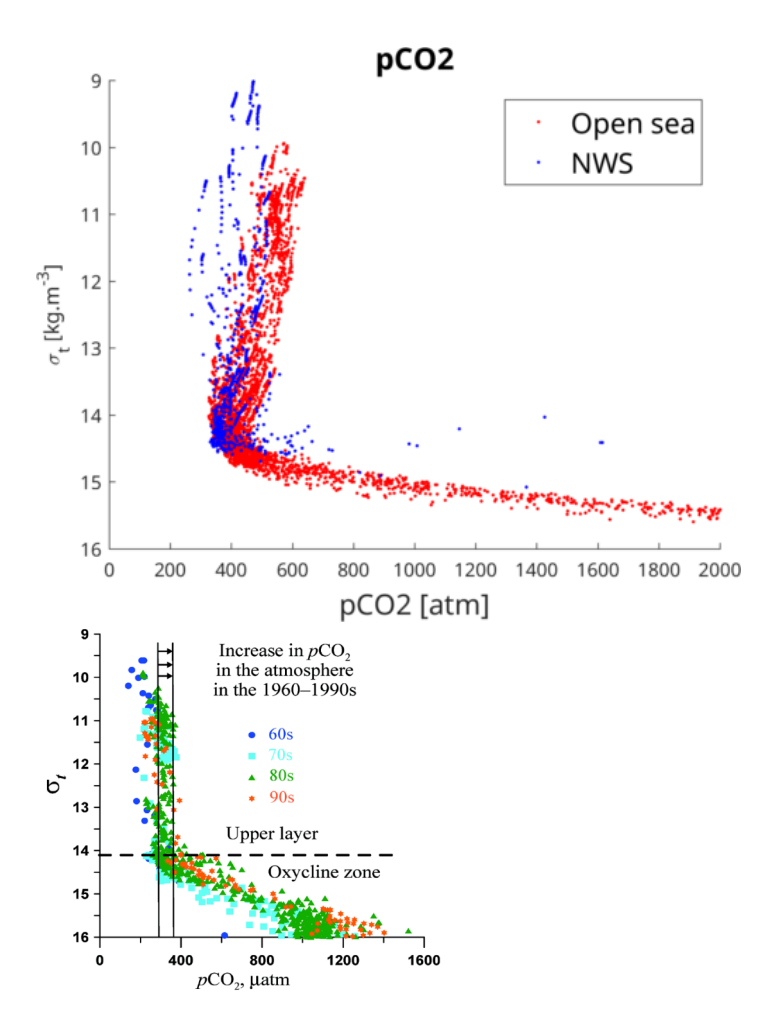


Figure 12: Comparison of model and observations of pCO2 as a function of the density anomaly. Left panel: CMEMS BS-MFC V202311 model (2021-2023). Right panel: observations, reprinted from Moiseenko et al. (2011).





Ref: Date: CMEMS-BLK-QUID-007-010

: September 2023

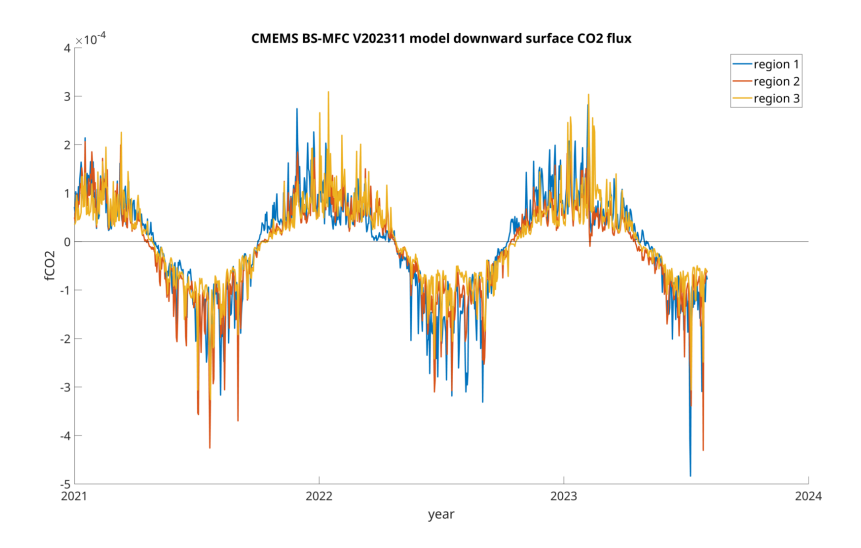
Issue: 4.0

V.5 Air-Sea CO2 Flux

Figure 13 shows time-series of spatially integrated (for each region) air-sea CO2 fluxes as obtained from the V202311 model. There are no available measurements of air-sea CO2 flux over the Black Sea open sea area for the validation period. Regarding the coastal areas, however, the modelled values in region 4 can be compared to the literature (Khoruzhiy, 2018) presenting values for 2011-2014. The modelled values are in a similar range as in Khoruzhiy (2018), and furthermore, they present a realistic seasonal variability.

The model at version V202311 uses time-varying atmospheric pCO2 values presenting seasonal and interannual variations, corresponding e.g. for 2022 to the $^{\sim}407$ -418 ppm range.

In the open sea, the annual mean of the CO_2 flux is upward (so the deep sea is a source of CO2 for the atmosphere), except in the Eastern basin where the temporal mean is approximately zero. In the NWS, at V202311, the annual mean of the CO2 flux is upward in regions 4 (Dniestr and Dniepr influenced), 5 (Danube influenced), 6 and 9 with the highest intensity on regions 4 and . Conversely, the flux is downward in regions 7, 8, 10 and 11.







Ref: CMEMS-BLK-QUID-007-010
Date: September 2023

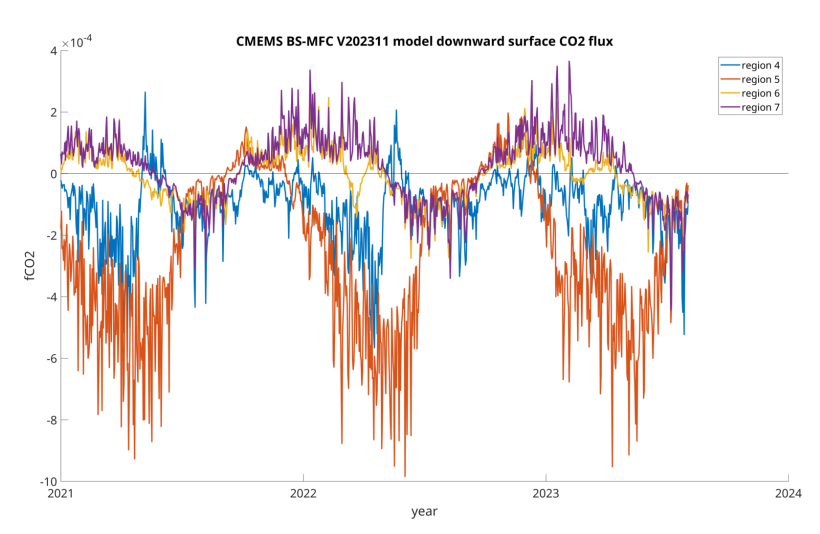


Figure 13: Time-series of modelled air-sea CO2 flux over the open sea regions (upper panel) and NWS regions (lower panel). The fluxes are positive downward, and are given in mmolC.m⁻².s⁻¹.





Ref:

CMEMS-BLK-QUID-007-010

Date: September 2023

Issue: 4.

V.6 Optics

The radiative forcing at the sea surface is computed in NEMO based on the date and time, latitude, and total cloud coverage. In BAMHBI, the solar surface radiation is split into its visible and infra-red parts, and the visible part is further partitioned into two bands: a short and a long component, using fixed proportions. The sea surface light is then propagated to depth taking into account the attenuation by seawater and by the optically-active biogeochemical components. The parameters that describe the light propagation (i.e. partitioning between a short and long component, absorption and backscattering coefficients) have been calibrated with vertical Photosynthetically Active Radiation (PAR) profiles. Finally, the daily average of the 3D light field is saved.

The validation of the optical product is done using (instantaneous) measurements of PAR and irradiation (at a wavelength of 490nm) by BGC-Argo floats, and of attenuation coefficients (Kd_{490}) from satellite products.

V.6.1 Photosynthetically Active Radiation (PAR)

The model delivers a daily-averaged profile of PAR while BGC-ARGO delivers instantaneous values. Therefore, the evaluation of the capacity of the model to propagate the light field along the vertical is realized by comparing a normalized PAR profile, obtained by dividing each measured and observed PAR profile data by its surface value. The surface PAR is evaluated by fitting an exponential curve into each observed profile. We thus compared the simulated and observed percentage of PAR attenuation. Observations obtained under skies with over 95% of total cloud coverage are rejected, as low-light conditions may result in low-quality observations. The cloud-coverage is estimated from ECMWF fields.

Since at a depths below 75 m, there is no more light (in both the model and observations), we decided to also compute the EANs only over the upper 75m.

The obtained EANs are shown in **Table 6**.

Table 6: Model skill statistics obtained by comparing model and BG-ARGO (see the position of the sites in **Figure 1**) predictions pairs for normalized PAR. Error metrics are defined in **Table 2**.

| PAR/PAR ₀ | all observations | upper 75 m |
|------------------------------------|------------------|------------|
| Bias [/] | -0.0071 | -0.019 |
| Percentage bias [%] | -24.16 | -19.86 |
| Rms [/] | 0.038 | 0.07 |
| Standard deviation ratio (no unit) | 1.15 | 1.14 |
| Nash-Sutcliffe (no unit) | 0.84 | 0.80 |
| Pearson coefficient (no unit) | 0.92 | 0.90 |

The EANs show an excellent correspondence of the normalized PAR between model and observations. Compared to V202211, the error statistics are slightly degraded.





Ref: CMEMS-BLK-QUID-007-010
Date: September 2023

Issue: 4.0

The distribution (over all measurements) of vertical normalized PAR profiles, and the corresponding model distribution, are shown in **Figure 14**. The small negative bias of the modelled normalized PAR compared to the observed one is visible (up to ~20 meter depth). The time-series of profiles for buoy 6903240 is shown in **Figure 15** as example.

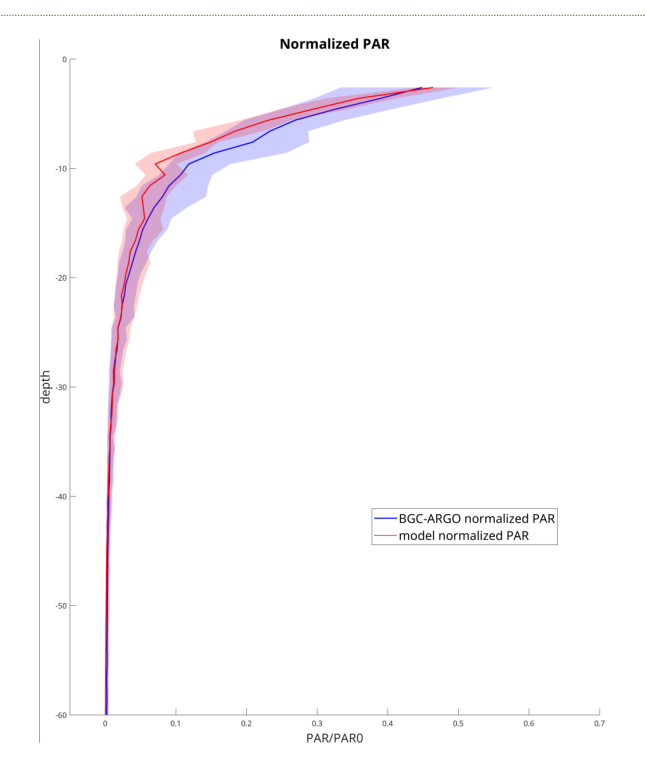


Figure 14: Normalized PAR. Blue: BGC-ARGO observation with depth (0 to -60 m). Red: NEMO-BAMHBI. The solid lines represent the median, the shaded areas cover percentiles 25% to 75%, over all observed profiles (locations represented in Fig. 1) over 2021-2022.

Commented [rvw20]: For next version, please can you make the axis labels in this plot larger? We cant read the text. Also for the curve labels.

Commented [rvw21]: For next version, please can you make the axis labels in this plot larger? We can hardly read the text. Also for the curve labels.





Ref: CMEMS-BLK-QUID-007-010 Date: September 2023

Issue:

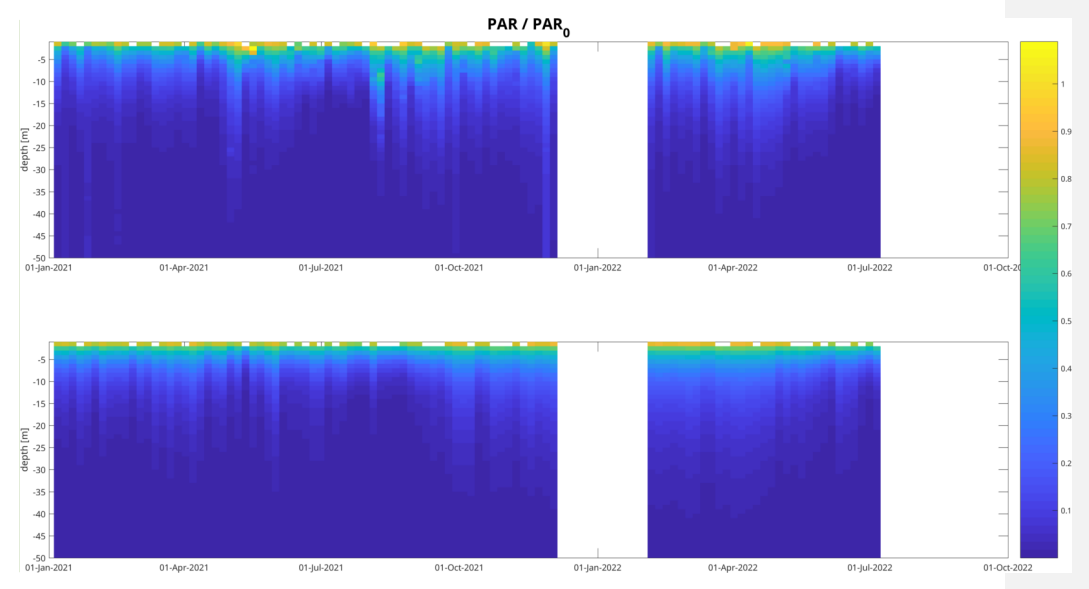


Figure 15: Hovmoller diagram of normalized PAR for buoy 6903240 during 2021-2022. Upper panel: BGC-Argo measurements. Lower panel: V202311 model equivalent.

V.6.2 Optical attenuation coefficient (Kd)

The model attenuation coefficients in each waveband (infrared, and short-and long-wavelengths of the visible light) are obtained by taking into account attenuation by seawater and by the various optically active biogeochemical components.

The BGC-Argo attenuation coefficients have been derived from downwelling irradiance profiles by fitting an exponential curve to the profile and then estimate Kd. The irradiance profiles are measured at different discrete wavelengths. Similarly, using satellite observations, the surface attenuation coefficients at different wavelengths are not directly observed but rather are derived at discrete wavelengths from the satellite reflectances.

Kd(490 nm) multi-satellite We delivered the product bv (OCEANCOLOUR_BS_OPTICS_L3_NRT_OBSERVATIONS_009_042). Since the BAMHBI model does not yet includes a spectral model, we use the modeled-derived attenuation coefficient derived in the short part of the PAR spectrum (wavelength between 400 and 580 nm). This is far from being perfect, but this Kd(short) is so far our best match with observed Kd(490).

Ocean color satellite products reflect what happens in the optical layer which is usually defined as the 1/Kd depth. Here, the model - satellite comparison is made over the first 5m of the water column.

Figure 16 shows the comparison for different regions (identified in Figure 1 of satellite Kd(490) and the modelled Kd(short) averaged over the surface layer. EANs are detailed below. Bias is around 0.03 m⁻¹ for mostregions, except regions 4 and 5. This is a strong increase compared to V202205, where the bias was around 0.003 $\,\mathrm{m}^{\text{-}1}$. Region 4 is the area influenced by the Dnestr and Dnepr rivers, (i.e. the Ukrainian shelf





Ref: CMEMS-BLK-QUID-007-010

Date: September 2023

Issue: 4

area) where the bias is around 0.23 $\,\mathrm{m}^{\text{-}1}$. The bias is 0.16 $\,\mathrm{m}^{\text{-}1}$ in the Danube-influenced region (region 5), which was not the case in V202105.

The surface Kd is well simulated in the deep basin during the winter months, where is presents almost no bias. During the summer months, in all regions the bias is large and positive (model attenuation is larger than satellite-estimated attenuation). This could partially be related to the arguments explained above, i.e. that model and observed Kd do not strictly represent the same wavebands, are not obtained over strictly the same depths. In the coastal regions except the ones in front of the Danube (regions 4 and 5), Kd biases are similar to the ones in the open sea. In regions 4 and 5, the EANs indicate a lower skill, most probably due to the very high variability of the optically active components in the Danube River plume (e.g. CDOMs, SPMs...), and the fact that the model misses real-time Danube discharge data for biogeochemical components (only real-time *water* discharge data are available).

BGC-ARGO floats measure the downwelling irradiance at different wavelengths (i.e. 380, 412, 490). We compare the modeled Kd(short) with Kd(490) from BGC ARGO which is the most representative wavelength of our model spectral band (400-580 nm); with 490 nm exactly the middle of the waveband (400-580 nm).

Kd(490) from BGC-Argo is estimated by first smoothing the downwelling irradiance delivered by Argo at 490 nm and then fitting a decreasing exponential (at each observed level). Without smoothing, the obtained attenuation profile would be extremely noisy with large jumps in value (over 100%) from one depth to the next.

Table 7 shows the error statistics obtained when comparing the modelled Kd(short) with the BGC Argo derived Kd(490) while **Figure 16** gives a comparison of vertical profiles. **Figure 17** When comparing the model with BGC-ARGO estimates of Kd, the EANs are improving compared to V202211.

It should be noted also that the surface estimate of Kd, obtained by BGC-ARGO, are quite different than the satellite estimates; biases are similar to the ones between model and satellite estimates.

Table 7: Model skill statistics obtained by comparing model and BG-ARGO predictions pairs for Kd (490). Error metrics are defined in **Table 2**.

| | bias | perc. bias | rms | std.dev ratio | Nash-Sutcliffe | Pearson |
|---------|------------------------|------------|----------------------|---------------|----------------|---------|
| V202211 | -0.034 m ⁻¹ | -26.9 % | 0.11 m ⁻¹ | 4.18 | 0.02 | 0.37 |
| V202311 | 0.017 m ⁻¹ | 16.22 % | 0.08 m ⁻¹ | 1.14 | 0.02 | 0.45 |

Commented [GM22]: Normal que ce soit négatif?

Commented [VL23]: oui, le biais a changé de signe entre V2022 et V2023





Ref: CMEMS-BLK-QUID-007-010

Date: September 2023

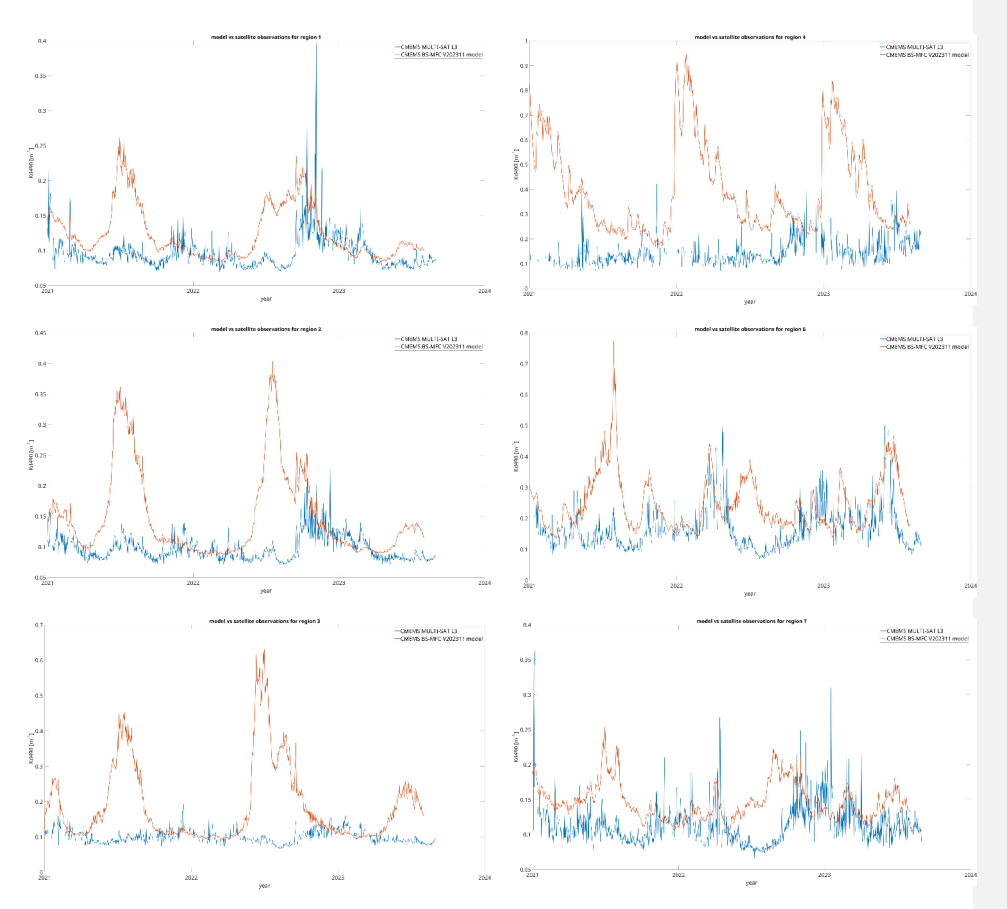


Figure 16: Time series of satellite (in blue) and model (in red) Kd spatial averages computed for (left column) open sea sub-regions 1, 2 and 3, and (right column) NWS regions 5, 6 and 7. The regions are shown in Figure 1.





Ref: CMEMS-BLK-QUID-007-010

Date: September 2023 Issue: 4.0

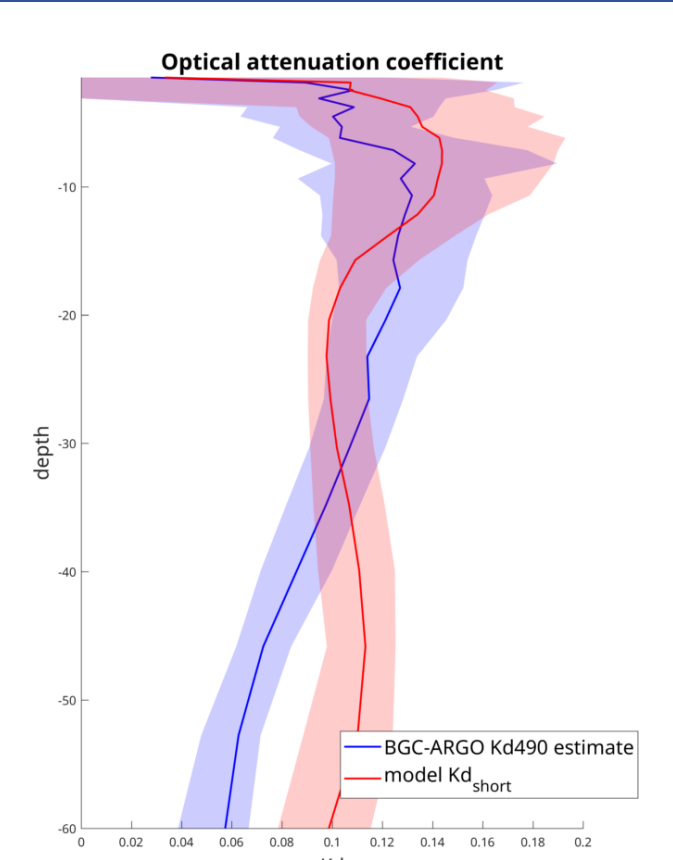


Figure 17: Blue: BGC-Argo Kd₄₉₀ estimated from irradiance. Red: NEMO-BAMHBI Kd₄₀₀₋₅₈₀. The solid line represents the median, the shaded area covers percentiles 25% to 75%, over all observed profiles (locations represented in **Figure 1**)





Ref: Date: CMEMS-BLK-QUID-007-010

September 2023

Issue: 4.0

VI SYSTEM'S NOTICEABLE EVENTS, OUTAGES OR CHANGES

N/A





Ref: CMEMS-BLK-QUID-007-010 Date: September 2023

Issue: 4.

VII QUALITY CHANGES SINCE PREVIOUS VERSION

As a reminder, the system at V201907 did undergo 2 major changes:

- The switch from the GHER to the NEMO v3.6 physical forcing model. The NEMO implementation is based on the BS-MFC-Physics model at V4, modified to better suit the biogeochemical forecasts.
- · The addition of an alkalinity module.

Then system at V202007 underwent the following changes:

- addition of data assimilation of satellite chlorophyll observations.
- change in the turbulence closure scheme and vertical diffusion coefficients.
- use of atmospheric pCO2 concentrations that vary in time following the inter-annual increase as indicated by the IPCC, as well as seasonally.

Next, the system at V202105 underwent the following change:

 addition of a new optics dataset containing 2 variables: photosynthetically active radiation (PAR) and optical attenuation coefficient (Kd).

At V202211, the system underwent the following changes:

- Switch from Nemo 3.6 to Nemo 4.0.6.
- Switch from 31 to 59 vertical levels.
- Usage of near real-time Danube fresh water discharge data from the NIHW (Romania)

Finally, at V202311, the following changes were implemented:

- Switch from Nemo 4.0.6 to Nemo 4.2
- New vertical discretisation, still using 59 z-layer levels, more dense between 50-150 meter depth, and coarser below. The surface layer still has 0.5m. The turbulence scheme is changed from TKE to GLSThe lateral diffusion is now computed using triads The surface heat exchange coefficients computation as a function of wind velocity is refined Chlorophyll is now a state variable (1 for each phytoplankton group) Refinement in the algorithm of the sinking speed of particulate organic matter The data assimilation scheme is based on a SEEK filter using 3D EOFs to construct a reduced-rank model state error space. However, similarly as spurious (horizontally) long-range correlations are suppressed, the correction is also limited in the vertical. This limitation is not static anymore, it is now computed as a function of the local mixed-layer depth.

VIII At V202311, the model configuration is exactly the same as for the corresponding multi-year product (007-005). The horizontal gris is also consistent with the PHY and WAV products. References

| Ref | Title | Date / Version |
|--------------------|---|----------------|
| CMEMS-PQ-MGT | CMEMS Product Quality Management Plan | Oct 2016 |
| Allen et al., 2007 | Allen, J. I., Somerfeld, P., Gilbert, F., 2007. Quantifying uncertainty in high- resolution coupled hydrodynamic-ecosystem models. <i>Journal of Marine</i> <i>Systems</i> , 64 (1-4), 3(14), contributions from Advances in Marine Ecosystem Modelling Research, 27-29 June, 2005, Plymouth, UK, AMEMR. | |





Ref: CMEMS-BLK-QUID-007-010
Date: September 2023

| Capet et al., 2016a | Decline of the Black Sea oxygen inventory. Biogeosciences 2016 | |
|-------------------------------|--|---|
| Capet et al., 2016b | Integrating sediment biogeochemistry into 3D oceanic models: A study of benthic-pelagic coupling in the Black Sea. Ocean Modelling, 2016 | |
| Capet et al., 2013. | Capet, A., Beckers, JM., & Grégoire, M. (2013). Drivers, mechanisms and long-term variability of seasonal hypoxia on the Black Sea northwestern shelf – is there any recovery after eutrophication? Biogeosciences, 10, 3943-3962 | |
| Capet, 2014 | Study of the multi-decadal evolution of the Black Sea hydrodynamics and biogeochemistry using mathematical modelling. PhD Thesis, Université de Liège, 2014 | |
| Geider et al, 1998 | Geiderl, Richard J., MacIntyre, Hugh L., Kana, Todd M., (1998), A dynamic regulatory model of phytoplanktonic acclimation to light, nutrients, and temperature, Limnology and Oceanography, 4, doi: 10.4319/lo.1998.43.4.0679. | |
| Gregoire et al., 2008. | Grégoire, M., Raick, C., & Soetaert, K. (2008). Numerical modeling of the deep Black Sea ecosystem functioning during the late 80's (eutrophication phase). Progress in Oceanography, 76(9), 286-333. | |
| Gregoire and Soetaert, 2010. | Grégoire, M., and Soetaert, K. (2010). Carbon, nitrogen, oxygen and sulfide budgets in the Black Sea: A biogeochemical model of the whole water column coupling the oxic and anoxic parts. Ecological Modelling, 15. | |
| Konovalov and Murray, 2001 | Konovalov, S. and J. Murray (2001). Variations in the chemistry of the Black Sea on a time scale of decades (1960–1995). Journal of Marine Systems, Vol 31, 217-243 | |
| Kopolevich et al., 2003 | Kopelevich O. V., S.V. Sheberstov, I.V. Sahling, S.V. Vazyulya, V.I. Burenkov (2013). Bio-optical characteristics of the Russian Seas from satellite ocean color data of 1998-2012. Proceedings of the VII International Conference "Current problems in Optics of Natural Waters (ONW 2013)", StPetersburg (Russia), September 10-14, 2013. | |
| Khoruzhiy, 2018 | D. Khoruzhiy, Variability of the CO2 Flux on the Water-Atmosphere Interface in the Black Sea Coastal Waters on Various Time Scales in 2010–2014, Physical Oceanography, 25(5), 2018 | |
| Joassin, 2011 | Joassin, P., 2011. Mathematical modeling of biogeochemical processes associated to a coccolithophorid (emiliania huxleyi) bloom - study of the seasonal and long-term variability of biogeochemical properties in the Black Sea using a data interpolating variational analysis (DIVA). Ph.D. thesis, Université de Liège. | |
| Maréchal, 2004. | Maréchal, D., 2004. A soil-based approach to rainfall-runoff modelling in ungauged catchments for England and Wales. PhD thesis, Cranfield University. 157 pp. | - |

| Ref | Title | Date / Version |
|-----------------------|---|----------------|
| Moiseenko et al, 2011 | O. Moiseenko, S. Konovalov, O. Kizlivskaya. Intraanuual and long-term variations of the carbonate system of the aerobic zone in the Black Sea. Physical Oceanogrpahy, Vol 20, 6, 2011 | |
| Ricour et al, 2021 | F. Ricour et al. Correction of in-situ fluorimetric measurements of chlorophyll-a concentrations in the Black Sea, BioGeoSciences, 2021 (in | |





Ref: CMEMS-BLK-QUID-007-010
Date: September 2023

| | press) | |
|--------------------|---|--|
| Stanev et al, 1997 | | |
| Vandenbulcke, 2015 | L. Vandenbulcke and A. Barth. The seamod.ro operational stochastic Black Sea forecasting system. Ocean Modelling, 2015 | |



